3D Metamaterials

Muamer Kadic[1,2], Graeme W. Milton[3], Martin van Hecke[4,5], and Martin Wegener[2]

Metamaterials are composites which are rationally designed, aiming at effective material parameters that go beyond (="meta", Greek) those of the ingredient materials. For example, negative metamaterial properties can result from positive-only ingredients. Likewise, large metamaterial parameter values can arise from all-zero constituents (*e.g.*, magnetic from non-magnetic, chiral from achiral, anisotropic from isotropic, etc.). Pushing the boundaries of accessible material behavior has been one of the driving forces of the metamaterial field. While the field emerged from linear electromagnetism two decades ago, it addresses nearly all conceivable aspects of solids today, ranging from electromagnetic/optical, mechanical/acoustic, to transport properties – linear and nonlinear, reciprocal and non-reciprocal, monostable and multistable ("programmable"), active and passive, as well as static and dynamic. Here, dynamic not only refers to frequency-dependent yet fixed material properties but to properties that actually change versus time *via* response to stimuli. In this Review, we focus on three-dimensional periodic metamaterials. We will outline fundamental bounds of these composites and summarize the state-of-the-art in theoretical design and experimental realization.

While the idea of artificial composite materials has been around for more than a century, the notion of three-dimensional (3D) metamaterials was coined only about twenty years ago [1]. Since then, the unprecedented experimental ability to tailor complex 3D architectures, the growing awareness of the exceptional effective properties of 3D metamaterials, and the tremendous progress in computer-aided design (including numerical forward solutions as well as inverse design, *e.g.*, *via* topology optimization [2]) have led to an explosion of interest. Many theorists and experimentalists have turned from observers of nature to creative designers and engineers of artificial materials. In many cases studied so far, the properties of 3D metamaterials go beyond those of their ingredients, both qualitatively and quantitatively. Examples include: negative refractive indices, dia- and paramagnetism at optical frequencies, gigantic optical activity, exceptionally large nonlinear optical suceptibilities, non-reciprocal behavior, negative mass densities, nontrivial mass density tensors, negative bulk moduli, negative acoustic indices, negative effective static volume compressibility, auxetic behavior, pentamode behavior, chiral and achiral micropolar behavior, multistable and programmable mechanical parameters, sign reversal of the thermal expansion coefficient, sign reversal of the Hall coefficient, and negative absolute mobilities. More examples are likely to emerge in the future.

Two decades after the 1999 publication by Rodger Walser [1] using the notion of "metamaterials" for the first time, we have still not arrived at a definition for metamaterials that is consistently used by all [3]. Most researchers would perhaps agree on the following "loose" definition:

Metamaterials are rationally designed composites made of tailored building blocks, which are composed of one or more constituent bulk materials. The metamaterial properties go beyond those of the ingredient materials – qualitatively or quantitatively.

Speaking of bulk material ingredients compresses much of the atomic complexity and implies that the metamaterial building blocks or unit cells contain millions of atoms or more (see Fig. 1(a,b,c)) [4]. This aspect makes metamaterials distinct from ordinary crystals. The above definition comprises periodic and non-periodic (see Fig. 1(e)) composites [5, 6]. We will focus on the periodic case, as the vast majority of metamaterials realized so far is actually periodic (Fig. 1(f)), and lattice translational invariance eases the discussion. Hence, the simplest example for a metamaterial is a single bulk material into which a rationally designed periodic porosity is introduced to achieve novel properties.

Rational design is a crucial aspect. It makes metamaterials distinct from, *e.g.*, random foams, patterns, or mixtures. By virtue of rational design of the structure, the metamaterial properties can go beyond those of the ingredients – both qualitatively and quantitatively [5]. The properties can even be unprecedented, not found in nature, or previously believed to be "impossible". Of course,

[1]Institut FEMTO-ST, UMR 6174, CNRS, Université de Bourgogne Franche-Comté, 25000 Besançon, France
[2]Institute of Nanotechnology and Institute of Applied Physics, Karlsruhe Institute of Technology (KIT), 76228 Karlsruhe, Germany
[3]Department of Mathematics, University of Utah, Salt Lake City, Utah 84112, USA
[4]AMOLF, Science Park 104, 1098 XG Amsterdam, the Netherlands
[5]Huygens-Kamerlingh Onnes Lab, Universiteit Leiden, PO Box 9504, 2300 RA Leiden, the Netherlands

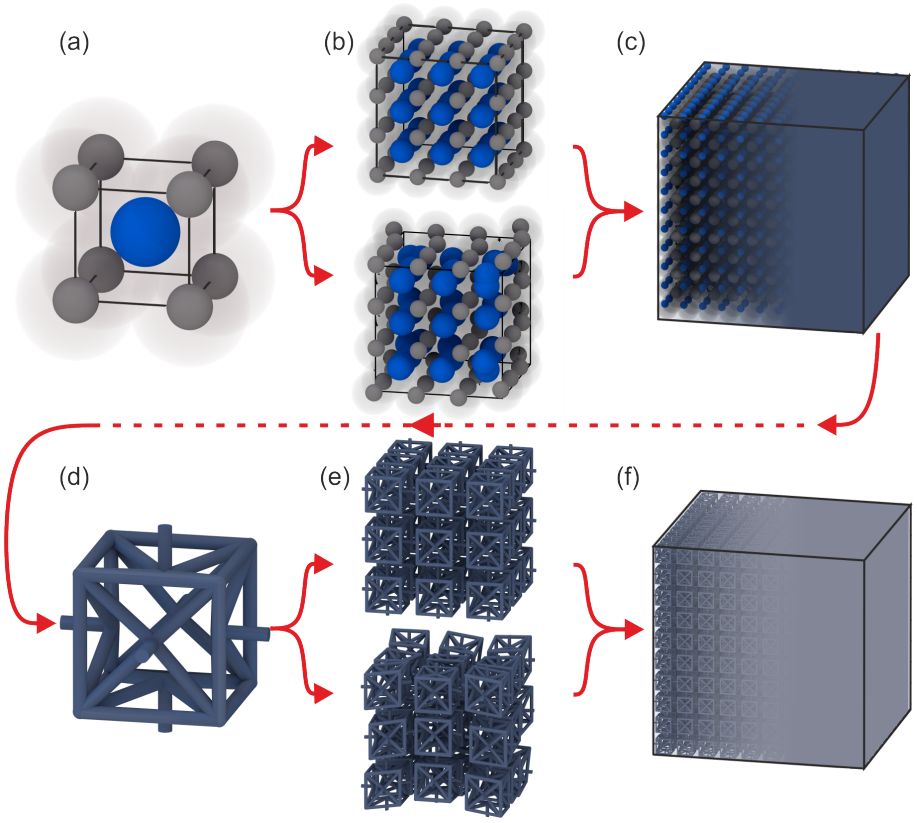

Figure 1. **From atoms via 3D materials to designed unit cells and 3D metamaterials.** (a) and (b) Ordinary crystalline or amorphous materials are built up from atoms. (c) To compress the underlying complexity, materials are often treated as fictitious continuous media with associated effective parameters such as the electric conductivity, the optical refractive index, or the mechanical Young's modulus. (d) These effective media are used as the ingredients for rationally designed artificial unit cells. (e) Out of these, periodic or non-periodic 3D metamaterials are assembled. (f) Again, to compress complexity, metamaterials are mapped onto fictitious continuous media. Notably, the resulting effective metamaterial properties can go beyond (= "meta", Greek) those of the ingredient materials, qualitatively and/or quantitatively. This includes, *e.g.*, the possibility of sign reversals and unbounded behavior. The example unit cell shown in (d) leads to auxetic behavior. Further examples are depicted in Figure 2.

truly fundamental bounds – which may be different for 1D, 2D, and 3D – cannot be overcome.

Effective parameters. Materials are commonly described by effective macroscopic material parameters referring to fictitious continua [5, 7]. Examples are the electric conductivity, the Hall coefficient, the electric permittivity, or the Young's modulus. In this manner, the complexity of a large system composed of many different materials can be reduced. With the addendum

> *. . . The properties of the metamaterial can be mapped onto effective-medium parameters.*

we sharpen our definition of metamaterials.

Homogenization theory [8–11] aims at providing a sound mathematical basis for mapping periodic structures onto effective media or continua. Notably, it is (presently) not possible to homogenize just any periodic structure and map it onto an effective-medium description, although high-frequency homogenization has been around for some years [7, 8, 12] and continues making progress in this direction [13]. Issues persist in regard to dealing with interfaces in an unambiguous way [11]. Homogenization becomes especially challenging in the limit that the material contrast of the ingredient materials is large or even diverges as the cell size shrinks to zero [14–16].

For many of the architectures to be dis-

cussed in this review, the mapping onto effective parameters is possible because some characteristic length scale, *e.g.*, the wavelength or a transport length, is sufficiently large compared to the period or lattice constant. Still, one should be aware that effective continuum descriptions are usually not perfect [17–19], not even for ordinary crystals. Furthermore, the mapping onto effective parameters is generally not unique. As a simple example, we can describe the optical properties of silicon either by a frequency-dependent conductivity or by a frequency-dependent complex refractive index. For other architectures discussed below, it is not yet clear whether homogenization is possible. However, researchers have improved and conceptually expanded homogenization theories over the years and are continuing to do so. Hence, a structure that cannot be mapped onto an effective medium today, may be tomorrow. For yet other periodic architectures, homogenization does not make sense. For example, it is generally problematic to map the complex band structure of a photonic [20] or phononic [21] crystal, which may even contain topological band gaps [22–24], onto effective material parameters – with the notable exception of the lowest bands in the long-wavelength limit.

Several other notions used in the literature are more or less synonymous to the notion of metamaterials, notably "architected materials" (mainly used in the context of mechanics), "designer matter", "artificial materials", or "properties on demand". Metamaterials can be periodic in 1D, in 2D ("metasurfaces" [25]) or in 3D. This Review focusses on 3D metamaterials.

We start historically with negative-index metamaterials and end with the exciting perspective of stimuli-responsive and space-time metamaterials. In between, however, this review is not organized chronologically, but rather aims at emphasizing analogies and dissimilarities between electromagnetic/optical, mechanical/acoustic, and transport metamaterials. We spare out designed inhomogeneous metamaterial distributions, which, for example, enable invisibility cloaks and counterparts thereof, as this extension would deserve a review article on its own [26].

Electromagnetic/optical metamaterials Sometimes, bounds believed to be fundamental are actually not. The field of optical metamaterials started like that: In their famous textbook [27] on electromagnetic continua, Landau and Lifshitz argue, based on an inequality containing the atomic lattice constant $a < 1\,\mathrm{nm}$, that the relative magnetic permeability at optical frequencies is close to unity, $\mu = 1$. In other words, the magnitude of the magnetic dipole density excited by the magnetic field of light is negligible. As a result, most optics textbooks essentially only deal with the relative electric permittivity ϵ_r, which describes an electric dipole density excited by the electric field of light.

One should be surprised: It is no problem to induce a current by a time-varying magnetic field *via* Faraday's law into a small coil with inductance L, made out of metallically conducting wire. The induced circulating current leads to a local magnetic dipole moment *via* Ampère's circuital law. This moment can be made large by building a resonant LC circuit out of the coil and a capacitance C. Densely packing many such circuits into a 3D metamaterial leads to a large positive magnetic permeability μ_r below the resonance frequency and to $\mu_\mathrm{r} < 0$ slightly above the resonance. Many of the metamaterial unit cells shown in Figure 2 include variations of this motif of a coil with one or more of slits, *i.e.*, a "split-ring resonator" [28, 29] (see Fig. 2(b)), also discussed in the literature under the names "slotted-tube resonator" [30], "loop-gap resonator" [31], or "cut-wire pairs" [32].

What prevents us from reaching optical frequencies? As the Maxwell equations are scalable, reducing the size by a factor of ten also reduces the resonance wavelength by the same factor, increasing the resonance frequency by a factor of ten. The answer lies in the finite electron density hence finite constituent metals plasma frequency, which is usually in the ultraviolet spectral region. When remotely approaching the plasma frequency, the metal properties deviate from those of an ideal conductor. The same physics can alternatively be expressed by the kinetic inductance [38], which adds to the Faraday inductance [39] and results in an upper limit of the LC frequency. In a circuit picture, further miniaturization towards the atomic scale is counterproductive, because the resistance R scales inversely with size, hence damping increases and the resonance gets washed out. This situation creates opportunities for metamaterials with lattice constants a much larger than the

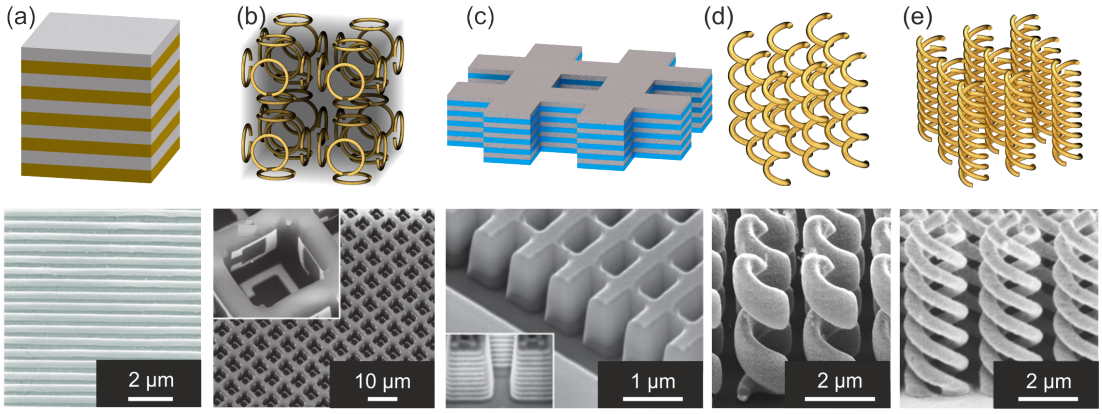

Figure 2. **Gallery of designed 3D optical metamaterial unit cells and corresponding experimental realisations.**| Classic unit cells used in all areas: (a) ABAB... laminate [33] Unit cell used in optics: (b) arrangement of metallic split-ring resonators leading to artificial magnetism [34], (c) fishnet arrangement for uniaxial negative refractive indices [35], (d) helices providing chiral behavior [36], and (e) multiple intertwined helices for recovering three-fold rotational symmetry [37].

atomic scale (compare Figure 1), yet smaller than the operation wavelength λ, such that the structure can approximately be described as an effective medium. Landau and Lifshitz [27] did not see that coming (Figure 2).

Negative refraction. The direction of the flow of light can be changed by refraction at an interface between two materials. The refractive index, n, in Snell's law determines this change. Unusual behavior can arise from negative n, from anisotropies, and from chirality.

A positive sign of n means that the vectors of phase velocity $\vec{v}_p$ and energy velocity $\vec{v}_e$ or Poynting vector $\vec{S}$ (which are generally not parallel to the group velocity vector [40]) point in the same direction ($\vec{v}_p \cdot \vec{S} > 0$), while they point in opposite directions if the refractive index is negative [41–46] ($\vec{v}_p \cdot \vec{S} < 0$). This situation, which can occur if the real parts of ϵ_r and μ_r are both negative [41, 42], is highly unusual (see Fig. 2(c)). It created much of the early excitement in the field of metamaterials, in large part due to the idea of "perfect lenses" [42] overcoming the Abbe diffraction barrier.

Causality imposes finite imaginary parts onto n, reflecting propagation losses. Mathematically, the Kramers-Kronig relations [47] derived from causality allow to obtain zero imaginary part of n at a single finite frequency of light by introducing gain media [48–51], but, unavoidably, losses quickly increase with increasing detuning from this singular point. In passive structures based on metallic constituents, the inferred ratio of negative real part to imaginary part, the so-called figure of merit, has not exceeded values on the order of ten at optical frequencies [35]. This means that the light intensity decreases by more than 70% over just one medium wavelength – *i.e.*, a bulk metamaterial with an extent of many wavelengths is essentially opaque. In addition, the few experimental studies actually considering 3D structures were mostly uniaxial, leading to anisotropic refractive index tensors, of which only components were negative. Related restrictions apply to zero-index and epsilon-near-zero metamaterials [52–54].

An alternative route to negative refraction are anisotropic materials [55]. Hyperbolic or indefinite [56–60] metamaterials (see Fig. 2(a)) are a special class of anisotropic media for which the electric permittivity is positive ("dielectric") along one direction and negative ("metallic") for the orthogonal one, leading to hyperbolic iso-frequency contours in momentum space. The hyperbola (in contrast to a circle or ellipse) gives access to large momenta of light, hence to unusually small effective wavelengths and "superresolution" at optical frequencies.

Optical magnetism. However, magnetism at elevated frequencies creates additional opportunities: $\mu_\mathrm{r} \neq 1$ allows for adjusting the electromagnetic wave impedance $Z = \sqrt{\mu_0 \mu_\mathrm{r}^* / (\epsilon_0 \epsilon_\mathrm{r}^*)}$ and make it equal to the vacuum impedance of $Z_0 = \sqrt{\mu_0/\epsilon_0} = 376\,\Omega$, independent of n. By impedance matching, reflections from interfaces between a mate-

rial and vacuum/air can thus be eliminated completely, regardless of the materials refractive index. Here losses, which have been a nuisance above, can be turned into an advantage in perfect absorbers: Materials that neither reflect nor transmit any light [61–64]. The idea of achieving impedance matching *via* balanced electric and magnetic responses is also key for the field of 2D Huygens metasurfaces [65]. For the case of $\mu_r^* < 0$ and $\epsilon_r^* > 0$, magnetic mirrors result [66] that ideally completely reflect the light, yet with a different phase shift than ordinary metal mirrors (where $\epsilon_r < 0$ and $\mu_r = 1$).

Cross couplings. So far, we have tacitly neglected chiral effects. Macroscopically, chiral effects such as, *e.g.*, optical activity, can be described by the dimensionless chirality parameter $\xi(\omega)$ [67, 68]. Microscopically, ξ summarizes that magnetic dipole moments are excited by the electric component of the electromagnetic light wave and *vice versa*. In the general anisotropic case, these "cross terms" are refered to as bianisotropy [67, 68]. We will encounter analogous couplings in Eringen continuum mechanics [69] below. These cross terms can only be nonzero if space inversion symmetry is broken. For light impinging under normal incidence onto a planar 2D system and emerging from it along the same axis, chiral effects are zero by symmetry [70]. Therefore, 3D metamaterials are of particular interest here.

As mentioned at the beginning of this section, chirality enables negative refractive indices *via* the relation $n_\pm^* = \sqrt{\epsilon_r^* \mu_r^*} \pm \xi^*$. Here, $\pm$ refers to left- and right-handed circular polarization, respectively. More interestingly, chiral 3D metamaterials can exhibit optical activity many orders of magnitude larger than what is found in natural substances. Furthermore, the wave impedance and the absorption coefficient also depend on the handedness of the circularly polarized light eigenstates. This allows for realizing circular polarizers [36], *i.e.*, materials that transmit one circular polarization of light and that reflect and/or absorb the opposite handedness nearly completely. 3D helical metallic metamaterials (see Fig. 2(d) and (e)) approach this ideal and even work over one to two octaves of bandwidth [37, 71, 72].

Recently, the concept of 3D metamaterials with extremal chirality was introduced [73]. Such media do not interact with one handedness of light impinging from vacuum/air at all, whereas they do interact (strongly) with the opposite one. This property is intimately connected to duality [73] ($\epsilon_r^* = \mu_r^*$. 3D metamaterials with extremal chirality have potential applications in angle-insensitive helicity-filtering glasses in stereoscopic 3D projection systems and in the optical sensing of chiral molecules [73, 74]. Such metamaterials can potentially be built exclusively from dielectric constituents. In essence, the Ohmic current in metals is replaced by the displacement current in dielectrics, leading to low losses.

If the excitation of magnetic dipoles by the electric field of light is not "symmetric" with respect to the excitation of electric dipoles by the magnetic field, a medium breaks time-reversal symmetry, becomes Faraday active, and behaves non-reciprocally. For a linear lossless stationary passive medium, this requires an internal or external static magnetic field. As one consequence, the transmission of light in one direction is no longer equal to the transmission in the opposite direction. For example, the bulky optical isolators in telecommunication systems are cost drivers and, hence, improved Faraday metamaterials would be highly welcome. Interesting steps in this direction have been taken [75]. This effect must not be confused with asymmetric polarization conversion, which is misleadingly sometimes referred to as "asymmetric transmission" [76]. We will come back to other options of breaking time-reversal symmetry in time-dependent and nonlinear media below.

Finally, to obtain any linear material response, one needs more than just electric and magnetic *dipole* moments. Toroidal moments have been discussed as a new multipole family for 3D optical metamaterials [77, 78]. However, reference [79] recently proved mathematically that electric and magnetic *multipole* moments suffice to capture all degrees of freedom for this purpose.

Nonlinearities. The combination of resonances, local-field enhancements, and local symmetry breaking has raised hopes for novel highly efficient nonlinear optical [80–82] and electro-optic 3D metamaterials [83, 84]. Indeed, novel geometries and record-high nonlinear optical susceptibilities have been reported [82], especially for the nonlinear refractive index, n_2, of metamaterials with $\epsilon_r \approx 0$, hence $n \approx 0$ [82]. However, it has also been pointed out [85] that 3D metamaterials and

theoretical blueprints for them have not improved compared to established nonlinear optical crystalline materials in regard to the figure-of-merit, *i.e.*, in terms of the accessible phase shift per absorption length or the accessible frequency-conversion efficiency per absorption length. Again, as for negative-index metamaterials, losses inherited from metallic ingredients are responsible [85]. Purely dielectric 3D metamaterials [82, 86, 87] generally exhibit less pronounced enhancements but might turn out to be more useful in practice [88].

Acoustic and mechanical metamaterials Let us start with the conceptually simplest case of airborn (or waterborn) acoustics. For acoustic waves in isotropic continua, the compressibility κ is mathematically analogous to the electric permittivity ϵ_r and the mass density ρ is analogous to the magnetic permeability μ_r [89]. Therefore, negative refractive indices can be obtained in acoustics in analogy to optics [90–93]. For example, a negative mass density at finite frequency $\omega \neq 0$ can be achieved slightly above a mass-and-spring resonance, where the instantaneous acceleration and force are 180 degrees out of phase [94] (see Fig. 3(b)). Taking different springs in the three spatial directions, the simple scalar mass density ρ can turn into a frequency-dependent rank-2 mass-density tensor $\rho(\omega)$ [95, 96]. 3D blueprints for such metamaterials [96–98] exploiting this freedom have been suggested theoretically (see [99]). Independent adjustment of the magnitudes of scalar $B(\omega)$ and $\rho(\omega)$ also enables acoustic impedance matching (analogous to optics above). Combined with finite absorption, perfect acoustic absorbers exhibiting zero reflection and zero transmission become possible [93]. For a single Lorentzian resonance, absorption can only be close to 100% over a limited frequency range. However, using a clever distribution of folded Fabry-Pérot resonators with different resonance frequencies in each unit cell, close to 100% absorption has been obtained experimentally over more than two octaves of frequency from 500-3000 Hz [100]. The absorber thickness of about 11 cm has been close to the fundamental limit determined by causality. Some of the authors have commercialized these 3D metamaterials for applications in noise reduction.

In acoustics, in contrast to optics, obtaining off-resonant moderately large positive refractive indices under meaningful conditions is not trivial [101]. Most solid materials have an acoustic impedance that is orders of magnitude larger than the impedance of air, such that close to 100% of the acoustic wave is reflected at the interface. Thereby, the phase velocity in the medium becomes irrelevant. Labyrinthine metamaterials [102, 103] (see Fig. 3(d)) can roughly match the acoustic impedance of air. Yet, by providing a winding detour by labyrinthine channels for sound inside of the unit cell bounded by rigid walls, on a scale much smaller than the acoustic wavelength, the phase velocity of the wave is effectively slowed down. Experiments have been reported for 2D [104, 105] and 3D metamaterials [103, 106].

An interesting twist which has no counterpart in electromagnetism is that the background air can also be actively driven in the channels of an acoustic metamaterial. This motion breaks reciprocity for the pressure wave propagating in the moving air. Metamaterials based on unit cells in which the air is locally circulating, driven by fans, have been demonstrated [114]. By constrictions in the channels, which locally modify the fluid motion, effectively gain and loss regions can be mimicked [115]. On this basis, metamaterials that are symmetric with respect to simultaneous space-inversion and time-inversion (PT-symmetric metamaterials) can be constructed [115].

Cauchy elasticity. The generalization of Hooke's law in one dimension to 3D solids led Cauchy to his elasticity tensor, $\boldsymbol{C}$, which connects stresses and strains [116]. The rank-4 Cauchy elasticity tensor is already much richer than the rank-2 electric permittivity tensor in optics. In a homogeneous isotropic medium, the permittivity tensor reduces to a scalar, whereas the elasticity tensor does not. It can be parameterized by two scalars though, *e.g.*, by the bulk modulus B, equal to the inverse of the compressibility κ, and the shear modulus G. Alternatively, one can use the Young's modulus E and the Poisson's ratio ν, or other combinations [116]. In an unconstrained stable passive medium under stationary conditions ($\omega = 0$), B and G cannot be negative. Likewise, a Hooke's spring constant cannot be negative. The bounds on other elastic parameters (such as E, ν, or the Lamé parameters) follow from that [117]. Intuitively, the difference in the rank of the

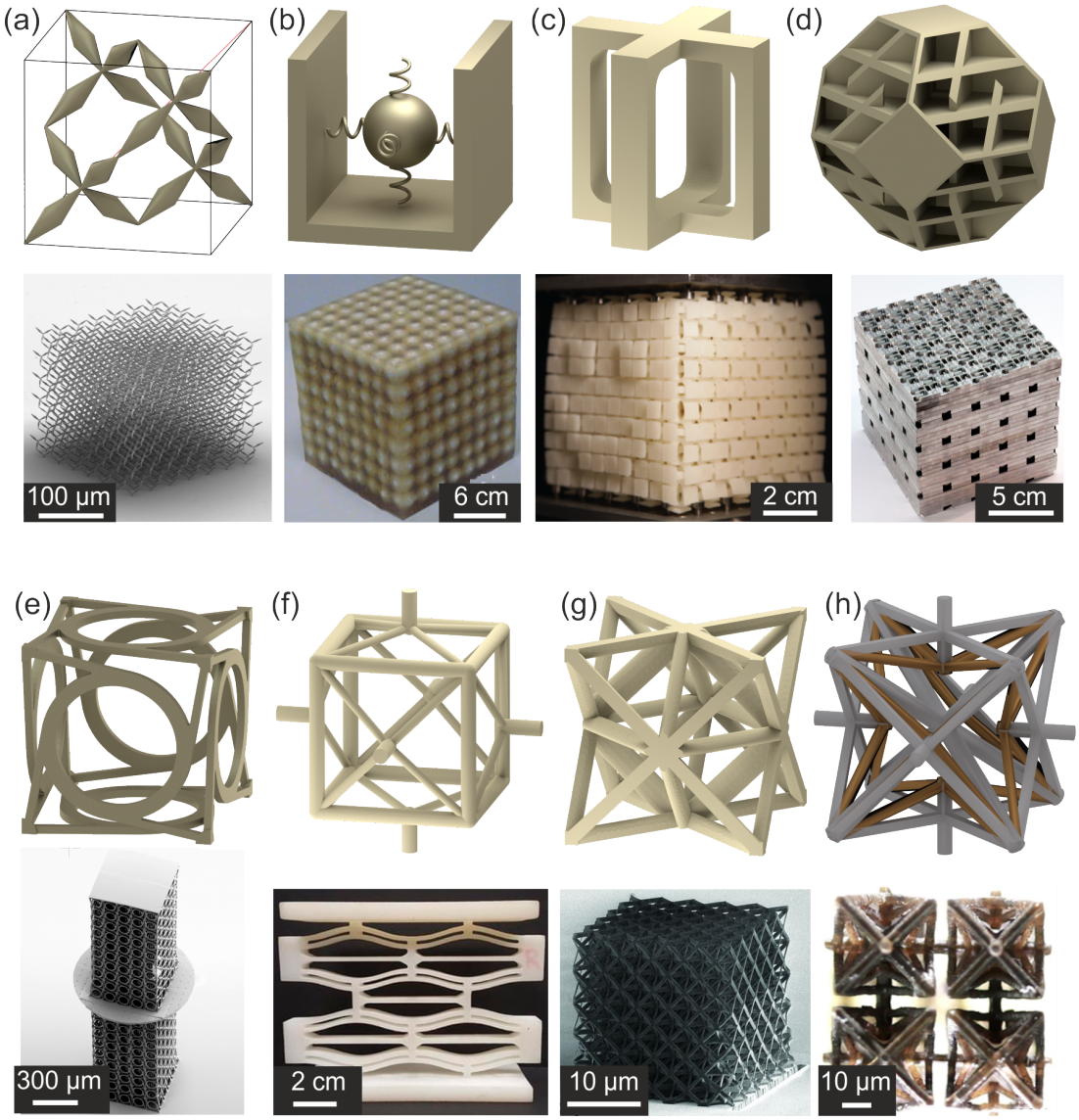

Figure 3. **Gallery of designed 3D acoustical and mechanical metamaterial unit cells and corresponding experimental realizations.**| Unit cells used in mechanics/acoustics: (a) pentamode cell leading to small shear modulus [107] (compare with auxetic cell in Figure. 1(d)) leading to small bulk modulus [108]), (b) internal mass-spring resonance leading to negative effective mass density [94], (c) programmable mechanical metamaterial [109], (d) 3D labyrinthine channel system leading to an isotropic slowing down of sound propagation [103], (e) 3D chiral mechanical metamaterial [110], (f) buckling elements leading to multistable and programmable behavior [111], and (g) truss lattices with large coordination number leading to strong ultralight behavior [112]. (h) Unit cells for stimuli-responsive behavior: two-component cell supporting sign reversal of thermal expansion [113].

tensors is connected to the fact that electromagnetism usually only supports transverse waves, whereas elasticity generally supports transverse and longitudinal waves at the same time. For the special case of acoustics, *e.g.*, with air or water as the medium, only the longitudinal pressure waves remain as the shear modulus is zero, $G = 0$ (see above).

For elastic solids, unlike air or water (see above), the shear modulus is generally not zero, $G \neq 0$. In auxetic elastic metamaterials, the effective shear modulus G^* can even be made larger than the effective bulk modulus, *i.e.*, $G^* > B^*$. Equivalently, the effective Poisson's ratio is negative, $\nu^* < 0$. Such materials contract laterally when pushing onto them (see Fig. 1(d)). For the limit of 3D isotropic dilational metamaterials with

$G^* \gg B^*$, we asymptotically get $\nu^* = -1$, which means that the only mode of material deformation is a change in volume without a change in shape of the material [118]. Thus, applications in shock protection by stress distribution are envisioned [118]. The opposite limit of $G^* \ll B^*$ brings us to pentamode metamaterials [119] (see Fig. 3(a)), which approximately behave as gases or liquids with $G = 0$, hence $\nu = 0.5$ (see above). 3D pentamodes [107] and anisotropic versions thereof [120] have been realized experimentally. Loosely speaking, pentamode metamaterials are more rubberish than rubber in the sense that the effective B/G-ratio can exceed 10^3. The soles composed of microlattices in the 3D printed shoes of a major sport manufacturer are related to this idea. Notably, the two limits of $\nu^* \to -1$ and $\nu^* \to +0.5$ are the only cases for which a cubic-symmetry 3D periodic metamaterial can generally be described by an isotropic Poisson's ratio [108]. Conceptually, all conceivable three-dimensional Cauchy elasticity tensors $\mathbf{C}$ can be constructed from pentamode materials [119].

Poroelastic metamaterials [121–123] combine much of the above: They support acoustic waves in their voids filled with air or a fluid and phonons in the elastic constituent solid. If these waves are phase matched, they can form mixed elastic-acoustic modes [15]. In the static regime, 3D cubic poroelastic metamaterials containing hollow inner volumes sealed by thin membranes have led to a negative static effective compressibility – for positive compressibility of both constituents, air and solid [123–125]. This means that the effective volume enclosed by the metamaterial surfaces increases when the surrounding hydrostatic air pressure increases. As the effective volume $V_{\text{eff}} = N\,a^3$ of N unit cells is not a thermodynamic quantity, this highly unusual sign reversal does not violate any law of physics.

Generalized elasticity. For linear optical metamaterials, we have started our discussion with the observation that most optics textbooks only deal with the electric permittivity tensor ϵ_{r} of continua and neglect magnetism at optical frequencies. For linear elastic mechanical materials, the situation is similar. Most standard textbooks [126] describe elastic continua on the level of Cauchy elasticity *via* the elasticity tensor $\boldsymbol{C}$, which connects stresses and strains [116], but neglects rotations. Again, the lattice constant a is a determining factor. If it is really small compared to all other relevant spatial scales (*i.e.*, wavelength and sample size), Cauchy elasticity is sufficient – just like the electric permittivity is sufficient for electromagnetic continua in the limit $a \to 0$, too (see above). Plainly speaking, the reason is that the rotation of a point-like object has no meaning. Therefore, electric fields in optics and displacements in mechanics are analogous. For intermediate metamaterial lattice constants a, however, an additional rotational field generally becomes important [69, 127]. This rotational field is analogous to the magnetic field of the light in optics. The analogy between optics and mechanics continues in that cross terms, *i.e.*, couplings between displacements and rotations, can occur for 3D chiral mechanical metamaterials [110, 128].

While all of these aspects are elements of Eringen's textbook micropolar continuum mechanics [69], they have only recently become experimental reality in the field of metamaterials [110, 128] (see Fig. 3(e)). In 3D chiral mechanical metamaterials, a pronounced conversion of a static axial push onto a beam into a twist of the beam was observed. This twist, which is forbidden in Cauchy elasticity, decayed only slowly with increasing number of unit cells in the beam [110, 128]. Some say that scalability is lost, because the properties depend on the size of the material and not only on the material itself. This notion has to be taken with some caution though: While certain behavior does depend on the number of unit cells in the metamaterial, the entries in the effective generalized Eringen elasticity tensors do *not* depend on size. The up to 12 independent moduli for cubic 3D micropolar metamaterials (196 for triclinic) are bounded in a complex way by reciprocity and the requirement that the eigenvalues cannot be negative [116]. In the dynamic case, 3D chiral phonons result [129]. In achiral 2D and 3D metamaterials, a related behavior was found [130]. There, for example, the effective static Hooke's spring constant does not double if one cuts a metamaterial beam into half [130]. A characteristic length scale over which Cauchy elasticity is recovered results from the elasticity tensors elements. This scale depends on the geometry of the metamaterial unit cell and can tend to infinity, such that Cauchy elasticity is eventually not recovered in the

large-sample limit [130, 131].

Recent theoretical work has yet gone one step further and considered gyroelastic metamaterials [5, 132–134] – the counterpart of Faraday active metamaterials in optics. A built-in continuously rotating gyroscope replaces the static magnetic field required in optics. Thereby, the mechanical metamaterial unit cell not only breaks space-inversion symmetry *via* chirality but also breaks time-inversion symmetry. This leads to an asymmetric cross-coupling between torques and displacements on the one hand, and between forces and rotations on the other hand, respectively [69, 127] (see optics above for comparison).

We should like to emphasize, however, that the generalizations of Cauchy elasticity discussed so far are not the only possible ones. The rotations in Eringen continuum mechanics are in a way perturbations to regular elasticity. By contrast, in "strain-gradient metamaterials" [135], some components of the effective elasticity tensor are zero, such that the main contribution is the strain gradient term [136–141]. Again, Cauchy elasticity is not recovered in the large-sample limit. Another generalization are Willis metamaterials [96]. There, stress also depends on acceleration, and momentum also depends on the displacement gradient, not just the velocity.

Nonlinearities. So far, we have focused on linear mechanics. However, nonlinearities play a tremendous role in engineering. We distinguish between reversibly nonlinear mechanical behavior, such as buckling instabilities [142–144], and irreversibly nonlinear behavior, such as failure or fracture of the constituent material(s).

While reversible nonlinearities are often only a minor correction to the linear behavior in optics, geometrical nonlinearities can be huge effects in mechanics – even if the constituent material behaves perfectly linear. The nonlinearities can be tailored by the metamaterial unit cell geometry. It has been proven by construction that essentially any nonlinear mechanical behavior can be achieved [145, 146]. Even multi-stable behavior is possible based on the buckling of beams. This classic mechanism is closely related to the "click" you hear when pushing onto the lid of a marmalade jar. Beyond a certain strain, the stress no longer increases but rather decreases. Assembling a 3D metamaterial (see Fig. 3(f)) out of such buckling beams, in parallel and in serial, couples them. Under strain control, the resulting behavior is nonlocal because the buckling of one beam influences beams far away as the displacements of all unit cells have to add up to the pre-described overall displacement. The resulting stress-strain behavior is multistable [143, 144, 147]. Upon loading and unloading such metamaterial, it does not follow the same path. This means that energy is irreversibly dissipated into heat during each cycle. As the constituent material can be purely linearly elastic in this process, the cycling is repeatable many times. Applications in terms of shock absorbers have been suggested [147]. The buckling beams can also be designed to be multi-stable by themselves. In this case, the 3D metamaterial has multiple stable states at zero external force. The different states generally have different linear elastic behavior [109]. Therefore, the elastic behavior can be programmed in this sense (also see Origami metamaterials [148–151]). Finally, in the nonlinear regime, *e.g.*, for a buckling metamaterial, the stress-strain curve, $\sigma(\epsilon)$, does not need to by symmetric with respect to pushing or pulling, i.e., $\sigma(-\epsilon) \neq -\sigma(\epsilon)$. This asymmetry in the nonlinear response for a 1D "fishbone" metamaterial has been interpreted in terms of static non-reciprocity [152]. In sharp contrast, in the linear elastic regime, the stress-strain curve for passive media must obey the condition $\sigma(-\epsilon) = -\sigma(\epsilon)$ – even for asymmetric structures.

With respect to irreversible mechanical failure and fracture, the idea of 3D light-weight metamaterials has sparked considerable interest [112, 145, 153–156]. When decreasing the volume filling fraction, f, of the constituent material, the effective mass density ρ^* obviously decreases proportionally, $\rho^* \propto f$. At the same time, the stiffness and the strength, the stress σ at failure, also decrease unavoidably. However, the scaling exponent η between effective strength σ and mass density, $\sigma^* \propto (\rho^*)^\eta$, can be influenced by the 3D metamaterial architecture [154, 155, 157]. It, *e.g.*, depends on whether the behavior is dominated by beam bending or stretching. Truss-based lattices with large coordination number (or structural connectivity) turn out to be favorable [157] (see Fig. 3(g)). Along these lines, 3D microlattices approaching the maximum possible theoretical strength have been

achieved [154–156]. All of these metamaterials are not scalable in the sense that their properties change if all unit cell dimensions are scaled down by the same factor. To avoid confusion, we emphasize that loss of scalability in the sense used here is distinct from that mentioned in the context of micropolar 3D metamaterials (see above).

Transport metamaterials

Being response functions (see above), simple transport coefficients such as the electric conductivity σ, the diffusivity D, and the thermal conductivity κ of passive (meta-)materials cannot be negative under stationary conditions (*i.e.*, $\omega = 0$) due to energy conservation and the second law of thermodynamics. The specific heat c of a stable material cannot be negative either. Therefore, parameter sign reversals of these quantities in analogy to the refractive index (see above) are not allowed. This rule does not apply to active metamaterials though (see counter-example given below).

Other stationary transport coefficients such as the Hall coefficient [158–160] A_{H}, the Ettingshausen coefficient P_{E}, the Seebeck coefficient S, the Peltier coefficient Π, and the relative magnetoresistance change $\Delta R/R$ can be positive or negative in the stationary regime [161]. While obtaining non-reciprocal behavior is a hot and demanding topic in optics, acoustics, and mechanics (see above), it is standard in transport due to the existence of semiconductor pn-diodes.

Additional bounds apply for composites. The isotropic Hall coefficient A_{H}^* of a 2D metamaterial, made of positive (negative) constituents, in a perpendicular magnetic field cannot be negative (positive) [159]. The same holds true for 3D hierarchical laminates [5]. In 3D structures beyond laminates, this restriction does not apply and parameter sign reversal is allowed [160, 162, 163]. The same reasoning analogously applies to the Ettingshausen coefficient P_{E}. For Hall-effect based magnetic-field sensors, which are, *e.g.*, used in the compass apps of many modern mobile phones, the modulus of the Hall mobility μ_{H}, which is given by the product $\mu_{\mathrm{H}} = A_{\mathrm{H}}\sigma$, determines the sensitivity and the signal-to-noise ratio of the sensor. In a metamaterial made of non-magnetic constituents, the effective isotropic Hall mobility μ_{H}^* is fundamentally bounded by the Hall mobilities of the constituents (up to a factor of two) [164]. This bound can be broken in the presence of additional tailored spatial distributions of static para- and diamagnetic constituents within the composite [164].

The dimensionless non-negative ZT-value, with $ZT = \sigma S^2 T/\kappa$ and the thermodynamic temperature T, is the commonly used figure-of-merit for devices aiming at efficient thermoelectric energy conversion [166]. It has been shown theoretically, that for an arbitrary composite in a small or zero magnetic field, the effective ZT^*-value cannot exceed the largest ZT-value of its constituents [166]. This technologically unfortunate bound can be broken in the presence of large magnetic fields though [166, 167] (complement of Fig. 4(a)). Furthermore, at least one of the constituents of the metamaterial has to have a strong thermoelectric response and another constituent has to have a strong Hall effect, *i.e.*, a large Hall mobility (see above). It has been argued though that the power factor (or conversion capacity) may be equally important technologically [168]. Power factors of thermoelectric materials, unlike the figure-of-merit, can be improved by orders of magnitude through metamaterials, *e.g.*, by lamination (see Fig. 2(a)) of two or more thermoelectric constituent materials.

Transport experiments. In analogy to optics and mechanics, passive laminates have led to anisotropic electrical, thermal, and diffusive transport, using isotropic constituent materials [5, 169], as well as to improved thermoelectric power factors [168] (see Fig. 4(b)).

Following an earlier theoretical suggestion, absolute negative mobility was shown in active 2D microfluidic systems (not called metamaterials then) [170]. There, micrometer-sized polystyrene beads always moved in a direction opposite to the net acting force as a result of an interplay between thermal noise, a periodic and symmetric microfluidic structure, and a biased alternating-current electric field [170].

Following preceding theoretical work [161], passive microstructures (not called metamaterials then) composed of Hall bars made out of a 3D layer of n-type GaAs, punctured by a square array of cylindrical voids in the xy-plane (see Fig. 4(a)), have led to a highly anisotropic effective classical magnetoresistance [161]. Its modulus at $T = 90$K was found to be as large as $\Delta R_{xx}/R_{xx} \approx 65\%$ at an in-plane magnetic field corresponding to

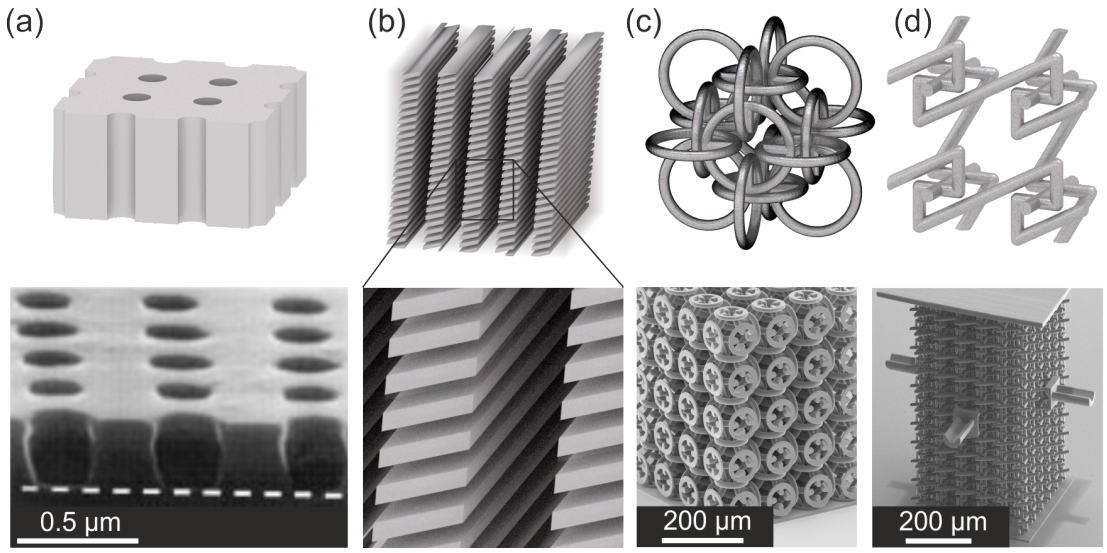

Figure 4. **Gallery of designed transport metamaterial unit cells and corresponding experimental realizations.**| (a) square array of cylindrical holes in a plate [161], leading to anisotropic, indefinite, or hyperbolic behavior. (b) hierarchical or Maxwell laminate. (c) chainmail-like arrangement of tori leading to sign reversal of the isotropic Hall coefficient [163] and (d) anisotropic cell supporting the parallel Hall effect [165].

$B_y = 12$ T [161]. In sharp contrast, the constituent GaAs crystal showed essentially zero magnetoresistance. In the strict 2D limit of a thin platelet, the magnetoresistance tends to zero theoretically [158]. Intuitively, the origin of the metamaterial magnetoresistance was interpreted in terms of a "geometrical shadow" of the current cast by the voids in the semiconductor along the direction of the magnetic field [161].

Following preceding theoretical work [159, 160, 162], a sign reversal of the effective 3D isotropic Hall coefficient with respect to the n-type ZnO constituent (*i.e.*, $\mathrm{sign}(A_\mathrm{H}^* A_\mathrm{H}) = -1$) has been observed [163] at room temperature in cubic symmetry chainmail-like metamaterials (see Fig. 4(c)), composed of interlinked hollow tori. The origin of this sign reversal can be traced back to the different topologies of a bulk material and a (hollow) torus made out of it [163]. Two further conceptually different paths to a sign reversal of A_H^* in 3D have been suggested theoretically [164]. They are based on exchanging the pick-up leads and reversing the local direction of the magnetic field, respectively, both in cubic symmetry. In lower symmetry metamaterials (see Fig. 2(d)), off-diagonal components of the Hall-tensor can dominate over the diagonal components [164]. Experiments on 3D metamaterials have shown the resulting unusual Hall voltage parallel (rather than perpendicular) to the external magnetic field [165] (see Fig. 4(d)). The parallel Hall effect could be used for sensors measuring the local circulation of a magnetic field [165]. It appears that any Hall tensor that is compatible with the Onsager relations [171] can be realized by 3D metamaterials composed of isotropic constituents [164]. However, a constructive proof for this conjecture is absent so far.

Stimuli-responsive metamaterials

The properties and associated effective-medium parameters of metamaterials are not necessarily fixed, they can be influenced by external stimuli and thereby be made to change deterministically versus time. This aspect requires that the constituent materials respond to some sort of stimulus, *e.g.*, to the local light intensity, or local electric field, magnetic field, pressure, temperature, etc. Liquid crystal displays are a widespread example. Here, the optical properties are changed by the application of electric fields which locally modulate the local liquid crystal orientation in each pixel. Using light as the stimulus for transparent metamaterials allows to selectively address individual unit cells in three dimensions, which tends to be difficult conceptually for other stimuli. 3D stimuli-responsive constituent materials are an ac-

tive field of research on their own [172–181]. Ideally, the metamaterial unit cell leverages these changes in some way, *e.g.*, by resonances or geometrical nonlinearities. Provided the metamaterial is multi-stable, the stimulus can even program the metamaterial in the sense that the reversibly induced change persists after the stimulus is being switched off. Table 1 gives an overview on the experimental status of stimuli-responsive and programmable metamaterials (see *e.g.* Fig. 3(c)), albeit not all in 3D. The columns refer to different material properties, the rows to different types of stimuli.

Stimulating all unit cells of a 3D metamaterial in the same way leads to tunable metamaterials, which could find applications as modulators. The metamaterial unit cells can be the same initially and then change in different ways, such that a specific functionality is induced by a stimulus [182–187]. Moreover, the time-dependent stimulation can be such that it creates a circulation of some property within one metamaterial unit cell. The axis associated to this circulation acts analogous to a static magnetic field in Faraday-active optical materials and can thus lead to nonreciprocal propagation (see above) of electromagnetic [188] or acoustic waves [114] in 2D metamaterial lattices made out of 3D unit cells.

In addition, the properties can vary not just in space but also in time. Rather than having a "unit-cell" of periodicity in space, one has a unit cell of periodicity in 4D space-time [179, 206, 207]. Modulation of material properties in time can be achieved by the external stimuli as discussed above. Many unusual behaviors are theoretically predicted in space-time metamaterials, although it should be emphasized that theory, so far, has focused on only one spatial dimension plus time. One aspect is that such metamaterials at rest in the laboratory frame can mimic the Doppler frequency shift for media moving in the laboratory frame when waves are reflected off their interface [208]. In addition, one can get artificial magnetic fields for photons with an artificial Lorentz effect so they travel along circular arcs [209]. Tilted band structures can provide unidirectional band gaps [210]. Furthermore, strikingly novel types of wave behavior are possible, referred to as field patterns. The material wave and the propagating wave are concentrated on a pattern, the field pattern. Macroscopically, the wave amplitude may blow-up exponentially or remain bounded according to whether one is in the case of broken or unbroken PT-symmetry (see above). In the unbroken case, the wake behind a wavefront does not die away, rather the material remains excited.

So far, however, the concept of space-time metamaterials is theoretical [211]. Experiments need to identify suitable stimuli-responsive mechanisms (see Table 1) with sufficiently small response times and corresponding constituent materials, allowing for the manufacturing of such architectures.

Conclusions and perspectives

3D metamaterials are rationally designed composites, aiming at effective material parameters that go beyond those of their bulk ingredients – qualitatively and/or quantitatively. While the interest exploded about twenty years ago, triggered by the advance of negative-index metamaterials, we should humbly admit that not all new ideas are good and that not all good ideas are new. More than a Century ago, Maxwell discussed laminates, providing an anisotropic response from isotropic ingredients. In 1920, Lindman investigated arrangements of metal helices, leading to a giant effective chiral response (optical activity) from achiral ingredients. The list goes on [5]. However, at least three things have changed. The rise of nanotechnology has enabled the making of optical metamaterials, composed of unit cells with sub-wavelength feature sizes. Furthermore, reliable 3D Additive Manufacturing on various spatial scales has enabled the fabrication of complex 3D architectures for electromagnetism, optics, acoustics, mechanics, and transport that seemed very difficult if not impossible to make twenty years ago. In parallel, we have seen significant progress and new approaches in theoretical design efforts, which could build on substantial advances in numerical computation and inverse design.

The metamaterial field can be proud. A long-standing dream of solid-state physics is to design materials on the computer, to avoid tedious trial-and-error procedures and excessive experimentation. However, the truth is that this dream has been realized in only few exceptions to date. Metamaterials are an entire class of such exceptions. A vast variety of highly unusual 3D metamaterial properties has been creatively *predicted* and then con-

Stimuli-responsive metamaterials	Electromagnetic stimuli	Mechanical stimuli	Thermodynamic stimuli
Optical/electromagnetic	[189–192]	[193, 194]	[195–197]
Mechanical/acoustical	[198, 199]	[109, 200]	[181, 201–203] (see Fig. 3h)
Transport properties	[197, 198]	[204]	[205]

Table I. **Stimuli-responsive metamaterials.**| Effective optical/electromagnetic, mechanical/acoustical, and transport properties can be influenced by optical, mechanical, and thermodynamic (temperature, hydrostatic pressure, and chemical potential) stimuli, leading to a "3×3-matrix" of possibilities. The upper two diagonal elements are the same as nonlinear optics and nonlinear mechanics, respectively. The nine entries are corresponding exemplary publications on metamaterials.

firmed experimentally.

Let us finally speculate about possible future perspectives of the field. At present, the number of researchers working on 2D metasurfaces is much larger than the number working on 3D metamaterials. It is argued that 2D structures are easier to fabricate, bringing the field closer to applications. Flat electromagnetic/optical metalenses are a prominent example. However, recent advanced metalenses use two or more layers to obtain additional degrees of freedom in the design process (in analogy to ordinary refractive-lens systems); otherwise, certain aberrations just cannot be corrected. This means that the 2D metasurface field is partly moving to 3D architectures. This step is not surprising in view of the fact that, conceptually, the possibilities of 2D structures are only a subset of the possibilities of 3D structures. Furthermore, 3D Additive Manufacturing has been rapidly progressing in recent years. In some years, 3D structures might be as easy to manufacture as 2D structures are today.

The connection between 3D metamaterials and 3D Additive Manufacturing, or loosely 3D printing, might become even tighter. A dream is to be able to 3D print "anything", including functional devices. Getting this ability will require realizing thousands of different optical, magnetic, mechanical, and transport material properties. Thousands of different input material cartridges are unlikely to be a viable solution. Today's 2D graphical ink-jet printers achieve thousands of different colors by mixing the inks from only 3 color cartridges. By analogy, based on microstructure rather than mixing, future 3D material printers may achieve thousands of different effective metamaterial properties starting from only a small number of input material cartridges. This review has illustrated many steps in this direction.

Acknowledgement
We acknowledge stimulating discussions with Carsten Rockstuhl (KIT). M.K. acknowledeges support by the EIPHI Graduate School (contract "ANR-17-EURE-0002") and the French Investissements d'Avenir program, project ISITE-BFC (contract ANR-15-IDEX-03). G.W.M. thanks the National Science Foundation for support *via* grant DMS-1211359 and DMS-1814854. M.W. acknowledges support by the Excellence Cluster "3D Matter Made to Order", the the Helmholtz program "Science and Technology of Nanosystems" (STN), the "Karlsruhe School of Optics & Photonics" (KSOP), and by the "Virtual Materials Design" (VIRTMAT) project of KIT.

References

[1] R. M. Walser, Inaugural Lecture, Proc. of SPIE, Complex Mediums II: Beyond Linear Isotropic Dielectrics; Lakhtakia, A, Weiglhofer, W.S., and Hodgkinson, I.J.editors **4467**, 1 (2001).
[2] M. Bendsøe and O. Sigmund, *Topology Optimization: Theory, Methods and Applications* (Springer, 2004).
[3] V. Browning, DARPATech 2002 **7**, 791–795 (2002).
[4] C. Kittel, *Introduction to Solid State Physics* (Wiley, 2004).
[5] G. W. Milton, *The Theory of Composites* (Cambridge University Press, 2002).
[6] K. Golden, G. Grimmett, R. James, G. Milton, and P. Sen, *Mathematics of Multiscale Materials*, The IMA Volumes in Mathematics and its Applications (Springer New York, 2012).
[7] R. V. Craster, J. Kaplunov, and A. V. Pichugin, Proc. R. Soc. London Ser. A **466**, 2341 (2010).
[8] A. Bensoussan, J. Lions, and G. Papan-

icolaou, *Asymptotic Analysis for Periodic Structures*, AMS Chelsea Publishing Series (American Mathematical Society, 2011).
[9] V. Jikov, G. Yosifian, S. Kozlov, and O. Oleinik, *Homogenization of Differential Operators and Integral Functionals*, SpringerLink : Bücher (Springer Berlin Heidelberg, 2012).
[10] N. Bakhvalov and G. Panasenko, *Homogenisation: Averaging Processes in Periodic Media: Mathematical Problems in the Mechanics of Composite Materials*, Mathematics and its Applications (Springer Netherlands, 2012).
[11] K. Pham, A. Maurel, and J.-J. Marigo, J. Mech. Phy. Solids **106**, 80 (2017).
[12] M. Brassart and M. Lenczner, J. Math. Pures Appl. **93**, 474 (2010).
[13] D. Harutyunyan, G. W. Milton, and R. V. Craster, Proc. R. Soc. London Ser. A **472** (2016).
[14] E. Y. Krushlov, Math. USSR Sbornik **35**, 266–282 (1979).
[15] J. L. Auriault and C. Boutin, Transport in Porous Med. **14**, 143 (1994).
[16] V. V. Zhikov, Mat. Sb. **191**, 31 (2010).
[17] J. B. Pendry, A. J. Holden, W. J. Stewart, and I. Youngs, Phys. Rev. Lett. **76**, 4773 (1996).
[18] P. A. Belov, R. Marqués, S. I. Maslovski, I. S. Nefedov, M. Silveirinha, C. R. Simovski, and S. A. Tretyakov, Phys. Rev. B **67**, 113103 (2003).
[19] C. Menzel, T. Paul, C. Rockstuhl, T. Pertsch, S. Tretyakov, and F. Lederer, Phys. Rev. B **81**, 035320 (2010).
[20] C. Soukoulis and M. Wegener, Nat. Photonics **5**, 523–530 (2011).
[21] V. Laude, *Phononic Crystals: Artificial Crystals for Sonic, Acoustic, and Elastic Waves*, De Gruyter Studies in Mathematical Physics (De Gruyter, 2015).
[22] C. L. Kane and T. C. Lubensky, Nat. Phys. **10**, 39–45 (2014).
[23] R. Süsstrunk and S. D. Huber, Science **349**, 47 (2015).
[24] R. Süsstrunk and S. D. Huber, Proc. Natl. Acad. Sci. USA PNAS **113**, E4767 (2016).
[25] H.-T. Chen, A. J. Taylor, and N. Yu, Rep. Prog. Phys. **79**, 076401 (2016).
[26] M. McCall *et al.*, J. Opt. **20**, 063001 (2018).
[27] L. D. Landau and E. M. Lifshitz, *Electrodynamics of continuous media*, Course of Theoretical Physics (Pergamon Press, 1960).
[28] S. A. Schelkunoff and H. T. Friis, *Antennas: the theory and practice* (pub-WILEY, 1952) pp. 584–585.
[29] J. B. Pendry, A. J. Holden, D. J. Robbins, and W. J. Stewart, IEEE Trans. Microw. Theory Tech. **47**, 2075 (1999).
[30] H. J. Schneider and P. Dullenkopf, Rev. Sci. Instrum. **48**, 68 (1977).
[31] B. T. Ghim, G. A. Rinard, R. W. Quine, S. S. Eaton, and G. R. Eaton, J. Magn. Reson. A **120**, 72 (1996).
[32] A. N. Lagarkov and A. K. Sarychev, Phys. Rev. B **53**, 6318 (1996).
[33] K. V. Sreekanth, A. D. Luca, and G. Strangi, Sci. Rep. **3**, 3291 (2013).
[34] D. B. Burckel, J. R. Wendt, G. A. T. Eyck, J. C. Ginn, A. R. Ellis, I. Brener, and M. B. Sinclair, Adv. Mater. **22**, 5053 (2010).
[35] J. Valentine, S. Zhang, T. Zentgraf, E. Ulin-Avila, D. A. Genov, G. Bartal, and X. Zhang, Nature **455**, 376–379 (2008).
[36] J. Gansel, M. Thiel, M. Rill, M. Decker, K. Bade, V. Saile, G. von Freymann, S. Linden, and M. Wegener, Science **325**, 1513 (2009).
[37] J. Kaschke and M. Wegener, Opt. Lett. **40**, 3986 (2015).
[38] A. Rose-Innes and E. Rhoderick, *Introduction to superconductivity*, International series in solid state physics (Pergamon Press, 1978).
[39] R. Meade, *Foundations of Electronics*, Foundations of Electronics, Circuits and Devices (Thomson/Delmar Learning, 2002).
[40] G. Dolling, C. Enkrich, M. Wegener, C. M. Soukoulis, and S. Linden, Science **312**, 892 (2006).
[41] V. Veselago, Sov. Phys. Usp. **10**, 4 (1968).
[42] J. B. Pendry, Phys. Rev. Lett. **85**, 3966 (2000).
[43] R. A. Shelby, D. R. Smith, and S. Schultz, Science **292**, 77 (2001).
[44] S. Zhang, W. Fan, N. C. Panoiu, K. J. Malloy, R. M. Osgood, and S. R. J. Brueck, Phys. Rev. Lett. **95**, 137404 (2005).
[45] C. M. Soukoulis, S. Linden, and M. Wegener, Science **315**, 47 (2007).
[46] C. García-Meca, J. Hurtado, J. Martí, A. Martínez, W. Dickson, and A. V. Zayats, Phys. Rev. Lett. **106**, 067402 (2011).
[47] P. Kinsler and M. W. McCall, Phys. Rev. Lett. **101**, 167401 (2008).
[48] N. I. Zheludev, S. L. Prosvirnin, N. Papasimakis, and V. A. Fedotov, Nature Photon. **2**, 351–354 (2008).
[49] M. A. Noginov, G. Zhu, A. M. Belgrave, R. Bakker, V. M. Shalaev, E. E. Narimanov, S. Stout, E. Herz, T. Suteewong, and U. Wiesner, Nature **460**, 1110–1112 (2009).
[50] A. Fang, T. Koschny, M. Wegener, and C. M. Soukoulis, Phys. Rev. B **79**, 241104 (2009).
[51] S. Wuestner, A. Pusch, K. L. Tsakmakidis, J. M. Hamm, and O. Hess, Phys. Rev. Lett. **105**, 127401 (2010).
[52] V. C. Nguyen, L. Chen, and K. Halterman, Phys. Rev. Lett. **105**, 233908 (2010).
[53] P. Moitra, Y. Yang, Z. Anderson, I. I. Kravchenko, D. P. Briggs, and J. Valentine, Nature Photon. **7**, 791–795 (2013).
[54] M. H. Javani and M. I. Stockman, Phys.

Rev. Lett. **117**, 107404 (2016).
[55] M. Wegener, G. Dolling, and S. Linden, Nat. Mater. **6**, 475–476 (2007).
[56] J. Yao, Z. Liu, Y. Liu, Y. Wang, C. Sun, G. Bartal, A. Stacy, and X. Zhang, Science **321**, 930 (2008).
[57] T. Cui, D. Smith, and R. Liu, *Metamaterials: Theory, Design, and Applications* (Springer US, 2009).
[58] H. N. Krishnamoorthy, Z. Jacob, E. Narimanov, I. Kretzschmar, and V. M. Menon, Science **336**, 205–209 (2012).
[59] V. M. García-Chocano, J. Christensen, and J. Sánchez-Dehesa, Phys. Rev. Lett. **112**, 144301 (2014).
[60] L. Ferrari, C. Wu, D. Lepage, X. Zhang, and Z. Liu, Prog. Quant. Electron. **40**, 1 (2015).
[61] N. I. Landy, S. Sajuyigbe, J. J. Mock, D. R. Smith, and W. J. Padilla, Phys. Rev. Lett. **100**, 207402 (2008).
[62] N. Liu, L. Langguth, T. Weiss, J. Kästel, M. Fleischhauer, T. Pfau, and H. Giessen, Nat. Mater. **8**, 758 (2009).
[63] C. M. Watts, L. Xianliang, and W. J. Padilla, Adv. Mater. **24**, 98 (2012).
[64] Y. Lee, J. Rhee, Y. Yoo, and K. Kim, *Metamaterials for Perfect Absorption*, Springer Series in Materials Science (Springer Singapore, 2016).
[65] C. Pfeiffer and A. Grbic, Phys. Rev. Lett. **110**, 197401 (2013).
[66] S. Liu, M. B. Sinclair, T. S. Mahony, J. C. Jun, S. Campione, J. Ginn, D. A. Bender, J. R. Wendt, J. F. Ihlefeld, P. G. Clem, J. B. Wright, and I. Brener, Optica **1**, 250 (2014).
[67] I. Lindell, *Electromagnetic Waves in Chiral and Bi-isotropic Media*, Antennas and Propagation Library (Artech House, 1994).
[68] S. Tretyakov, A. Sihvola, A. Sochava, and C. Simovski, J. Electromagnet. Wave **12**, 481 (1998).
[69] A. Eringen, *Elastodynamics*, Elastodynamics No. vol. 2 (Academic Press, 1974).
[70] M. Wegener and S. Linden, *Bi-anisotropic and Chiral Metamaterials* (Book chapter in Tutorials in Metamaterials, edited by M. A. Noginov and V. A. Podolskiy, Taylor and Francis Group, 2012).
[71] J. K. Gansel, M. Latzel, A. Frölich, J. Kaschke, M. Thiel, and M. Wegener, Appl. Phys. Lett. **100**, 101109 (2012).
[72] K. Johannes, B. Leonard, W. Lin, T. Michael, B. Klaus, Y. Zhenyu, and W. Martin, Adv. Opt. Mater. **3**, 1411 (2015).
[73] I. Fernandez-Corbaton, M. Fruhnert, and C. Rockstuhl, Phys. Rev. X **6**, 031013 (2016).
[74] Y. Lefier, R. Salut, M. A. Suarez, and T. Grosjean, Nano Lett. **18**, 38 (2018).
[75] J. Y. Chin, T. Steinle, T. Wehlus, D. Dregely, T. Weiss, V. I. Belotelov, B. Stritzker, and H. Giessen, Nat. Commun. **4**, 1599 (2013).
[76] V. A. Fedotov, P. L. Mladyonov, S. L. Prosvirnin, A. V. Rogacheva, Y. Chen, and N. I. Zheludev, Phys. Rev. Lett. **97**, 167401 (2006).
[77] T. Kaelberer, V. Fedotov, N. Papasimakis, D. Tsai, and N. Zheludev, Science **330**, 1510 (2010).
[78] N. Papasimakis, V. A. Fedotov, V. Savinov, T. A. Raybould, and N. I. Zheludev, Nat. Mater. **15**, 263–271 (2016).
[79] S. N. Ivan Fernandez-Corbaton and C. Rockstuhl, Sci. Rep. **7**, 7527 (2017).
[80] M. Wegener, *Extreme nonlinear optics* (Springer-Verlag, 2005).
[81] M. K. . A. V. Zayats, Nature Photon. **6**, 737–748 (2012).
[82] J. Lee, M. Tymchenko, C. Argyropoulos, P.-Y. Chen, F. Lu, F. Demmerle, G. Boehm, M.-C. Amann, A. Alù, and M. A. Belkin, Nature **511**, 65–69 (2014).
[83] Z. L. Sámson, K. F. MacDonald, F. De Angelis, B. Gholipour, K. Knight, C. C. Huang, E. Di Fabrizio, D. W. Hewak, and N. I. Zheludev, Appl. Phys. Lett. **96**, 143105 (2010).
[84] O. Buchnev, J. Y. Ou, M. Kaczmarek, N. I. Zheludev, and V. A. Fedotov, Opt. Express **21**, 1633 (2013).
[85] J. B. Khurgin and G. Sun, Opt. Express **21**, 27460 (2013).
[86] S. Jahani and Z. Jacob, Nature Nanotech. **11**, 23–36 (2016).
[87] I. Staude and J. Schilling, Nature Photon. **11**, 274–284 (2017).
[88] A. Hermans, C. Kieninger, K. Koskinen, A. Wickberg, E. Solano, J. Dendooven, M. Kauranen, S. Clemmen, M. Wegener, C. Koos, and R. Baets, Sci. Rep. **7**, 44581 (2017).
[89] M. Kadic, T. Bückmann, R. Schittny, and M. Wegener, Rep. Prog. Phys. **76**, 126501 (2013).
[90] Y. Ding, Z. Liu, C. Qiu, and J. Shi, Phys. Rev. Lett. **99**, 093904 (2007).
[91] S. H. Lee, C. M. Park, Y. M. Seo, Z. G. Wang, and C. K. Kim, Phys. Rev. Lett. **104**, 054301 (2010).
[92] Y. Wu, Y. Lai, and Z. Q. Zhang, Phys. Rev. Lett. **107**, 105506 (2011).
[93] S. A. Cummer, J. Christensen, and A. Alu, Nat. Rev. Mater. **1**, 16001 (2016).
[94] Z. Liu, X. Zhang, Y. Mao, Y. Y. Zhu, Z. Yang, C. T. Chan, and P. Sheng, Science **289**, 1734 (2000).
[95] M. Schoenberg and P. N. Sen, **73**, 61 (1983).
[96] G. W. Milton, New J. Phys. **9**, 359 (2007).
[97] J. R. Willis, Proc. Roy. Soc. London A **467**, 1865 (2011).
[98] M. B. Muhlestein, C. F. Sieck, P. S. Wil-

son, and M. R. Haberman, Nat. Commun. **8**, 15625 (2017).
[99] T. Bückmann, M. Kadic, R. Schittny, and M. Wegener, physica status solidi (b) **252**, 1671 (2015).
[100] M. Yang, S. Chen, C. Fu, and P. Sheng, Mater. Horiz. **4**, 673 (2017).
[101] G. Ma and P. Sheng, Sci. Adv. **2**, e1501595 (2015).
[102] Z. Liang and J. Li, Phys. Rev. Lett. **108**, 114301 (2012).
[103] T. Frenzel, J. D. Brehm, T. Bückmann, R. Schittny, M. Kadic, and M. Wegener, Appl. Phys. Lett. **103**, 061907 (2013).
[104] Y. Xie, A. Konneker, B.-I. Popa, and S. A. Cummer, Appl. Phys. Lett. **103**, 201906 (2013).
[105] A. O. Krushynska, F. Bosia, M. Miniaci, and N. M. Pugno, New J. Phys. **19**, 105001 (2017).
[106] S. K. Maurya, A. Pandey, S. Shukla, and S. Saxena, Sci. Rep. **6**, 33683 (2016).
[107] M. Kadic, T. Bückmann, N. Stenger, M. Thiel, and M. Wegener, Appl. Phys. Lett. **100**, 191901 (2012).
[108] T. Bückmann, R. Schittny, M. Thiel, M. Kadic, G. W. Milton, and M. Wegener, New J. Phys. **16**, 033032 (2014).
[109] C. Coulais, E. Teomy, K. de Reus, Y. Shokef, and M. van Hecke, Nature **535**, 529–532 (2016).
[110] T. Frenzel, M. Kadic, and M. Wegener, Science **358**, 1072–1074 (2017).
[111] D. Correa, T. Klatt, S. Cortes, M. Haberman, D. Kovar, and C. Seepersad, Rapid Prototyping Journal **21**, 193 (2015).
[112] L. R. Meza, S. Das, and J. R. Greer, Science **345**, 1322 (2014).
[113] Q. Wang, J. A. Jackson, Q. Ge, J. B. Hopkins, C. M. Spadaccini, and N. X. Fang, Phys. Rev. Lett. **117**, 175901 (2016).
[114] R. Fleury, D. L. Sounas, C. F. Sieck, M. R. Haberman, and A. Alu, Science **343**, 516 (2014).
[115] Y. Aurégan and V. Pagneux, Phys. Rev. Lett. **118**, 174301 (2017).
[116] B. Banerjee, *An Introduction to Metamaterials and Waves in Composites* (Taylor and Francis, 2011).
[117] L. Walpole, J. Mech. Phy. Solids **14**, 151 (1966).
[118] G. W. Milton, J. Mech. Phy. Solids **61**, 1543 (2013).
[119] G. W. Milton and A. V. Cherkaev, J. Eng. Mater.-T. **117**, 483 (1995).
[120] M. Kadic, R. Schittny, T. Bückmann, and M. Wegener, New J. Phys. **15**, 023029 (2013).
[121] M. Biot, J. Acoust. Soc. Am. **28**, 168–178 (1956).
[122] M. Biot and D. Willis, J. Appl. Mech. **24**, 594–601 (1957).
[123] R. Gatt and J. N. Grima, Phys. Stat. Sol. RRL **2**, 236 (2008).
[124] J. Qu, M. Kadic, and M. Wegener, Appl. Phys. Lett. **110**, 171901 (2017).
[125] J. Qu, A. Gerber, F. Mayer, M. Kadic, and M. Wegener, Phys. Rev. X **7**, 041060 (2017).
[126] A. Sommerfeld, *Mechanics of deformable bodies*, Lectures on theoretical physics (Academic Press, 1950).
[127] A. Eringen and G. Maugin, *Electrodynamics of Continua I: Foundations and Solid Media* (Springer New York, 2012).
[128] Z. Rueger and R. S. Lakes, Phys. Rev. Lett. **120**, 065501 (2018).
[129] H. Zhu, J. Yi, M.-Y. Li, J. Xiao, L. Zhang, C.-W. Yang, R. A. Kaind, L.-J. Li, and X. Z. Yuan Wang and, Science **359**, 579 (2018).
[130] C. Coulais, C. Kettenis, and van Hecke M, Nat. Phys. **14**, 40 (2017).
[131] M. Kadic, T. Frenzel, and M. Wegener, Nat. Phys. **14**, 8 (2018).
[132] L. M. Nash, D. Kleckner, A. Read, V. Vitelli, A. M. Turner, and W. T. M. Irvine, Proceedings of the National Academy of Sciences **112**, 14495 (2015).
[133] S. Hassanpour and G. R. Heppler, Acta Mechanica **227**, 1469 (2016).
[134] G. Carta, I. S. Jones, N. V. Movchan, A. B. Movchan, and M. J. Nieves, Sci. Rep. **7**, 26 (2017).
[135] H. Abdoul-Anziz and P. Seppecher, Archives-ouvertes **6**, 213 (2018).
[136] P. Gudmundson, J. Mech. Phys. Solids **52**, 1379 (2004).
[137] M. Olive and N. Auffray, J. Appl. Math. Mech. **94**, 421–447 (2014).
[138] N. M. Cordero, S. Forest, and E. P. Busso, J. Mech. Phys. Solids **97**, 92 (2016).
[139] C. Liebold and W. H. Müller, Computational Materials Science **116**, 52 (2016).
[140] G. Lecoutre, N. Daher, M. Devel, and L. Hirsinger, Acta Mechanica **228**, 1681 (2017).
[141] A. Bertram, Compendium on Gradient Materials, TU Berlin.
[142] P. Wang, F. Casadei, S. Shan, J. C. Weaver, and K. Bertoldi, Phys. Rev. Lett. **113**, 014301 (2014).
[143] B. Florijn, C. Coulais, and M. van Hecke, Phys. Rev. Lett. **113**, 175503 (2014).
[144] S. H. Kang, S. Shan, A. Košmrlj, W. L. Noorduin, S. Shian, J. C. Weaver, D. R. Clarke, and K. Bertoldi, Phys. Rev. Lett. **112**, 098701 (2014).
[145] J. Bauer, L. R. Meza, T. A. Schaedler, R. Schwaiger, X. Zheng, and L. Valdevit, Adv. Mater. **29** (2017).
[146] J. C. Katia Bertoldi, Vincenzo Vitelli and M. van Hecke, Nature Reviews Materials **2**, 17066 (2017).
[147] F. Tobias, F. Claudio, K. Muamer, G. Peter, and W. Martin, Adv. Mater. **28**, 5865.
[148] M. Schenk and S. D. Guest, Proc. Natl.

Acad. Sci. USA **110**, 3276 (2013).
[149] Z. Y. Wei, Z. V. Guo, L. Dudte, H. Y. Liang, and L. Mahadevan, Phys. Rev. Lett. **110**, 215501 (2013).
[150] S. Waitukaitis, R. Menaut, B. G.-g. Chen, and M. van Hecke, Phys. Rev. Lett. **114**, 055503 (2015).
[151] J. L. Silverberg, J.-H. Na, A. A. Evans, B. Liu, T. C. Hull, C. D. Santangelo, R. J. Lang, R. C. Hayward, and I. Cohen, Nat. Mater. **14**, 389 (2015).
[152] C. Coulais, D. Sounas, and A. Alù, Nature **542**, 461–464 (2017).
[153] H. Gao, B. Ji, I. L. Jäger, E. Arzt, and P. Fratzl, Proc. Nat. Acad. Sci. USA **100**, 5597 (2003).
[154] T. A. Schaedler, A. J. Jacobsen, A. Torrents, A. E. Sorensen, J. Lian, J. R. Greer, L. Valdevit, and W. B. Carter, Science **334**, 962 (2011).
[155] X. Zheng, H. Lee, T. H. Weisgraber, M. Shusteff, J. DeOtte, E. B. Duoss, J. D. Kuntz, M. M. Biener, Q. Ge, J. A. Jackson, S. O. Kucheyev, N. X. Fang, and C. M. Spadaccini, Science **344**, 1373 (2014).
[156] J. Bauer, S. Hengsbach, I. Tesari, R. Schwaiger, and O. Kraft, Proc. Nat. Acad. Sci. USA **111**, 2453 (2014).
[157] J. Bauer, R. Meza Lucas, T. A. Schaedler, R. Schwaiger, X. Zheng, and L. Valdevit, Adv. Mater. **29**, 1701850 (2002).
[158] R. S. Popovic, *Hall Effect Devices* (Institute of Physics Publishing, Bristol, Philadelphia, 2004).
[159] M. Briane, G. W. Milton, and V. Nesi, Arch. Rational Mech. Anal. **173**, 133 (2004).
[160] M. Briane and G. W. Milton, SIAM J. Appl. Math. **70**, 1810 (2010).
[161] M. Tornow, D. Weiss, K. von Klitzing, K. Eberl, D. J. Bergman, and Y. M. Strelniker, Phys. Rev. Lett. **77**, 147 (1996).
[162] M. Kadic, R. Schittny, T. Bückmann, C. Kern, and M. Wegener, Phys. Rev. X **5**, 021030 (2015).
[163] C. Kern, M. Kadic, and M. Wegener, Phys. Rev. Lett. **118**, 016601 (2017).
[164] C. Kern, W. M. Graeme, M. Kadic, and M. Wegener, New J. Phys. **20**, 083034 (2018).
[165] C. Kern, V. Schuster, M. Kadic, and M. Wegener, Phys. Rev. Applied **7**, 044001 (2017).
[166] D. J. Bergman and Y. M. Strelniker, Phys. Rev. B **49**, 16256 (1994).
[167] Y. M. Strelniker and D. J. Bergman, Phys. Rev. B **96**, 235308 (2017).
[168] L. Liu, New J. Phys. **16**, 123019 (2014).
[169] R. Schittny, M. Kadic, S. Guenneau, and M. Wegener, Phys. Rev. Lett. **110**, 195901 (2013).
[170] A. Ros, R. Eichhorn, J. Regtmeier, T. T. Duong, P. Reimann, and D. Anselmetti, Nature **436**, 928 (2005).
[171] L. Onsager, Phys. Rev. **37**, 405 (1931).
[172] J. D. Debord and L. A. Lyon, The Journal of Physical Chemistry B **104**, 6327 (2000).
[173] M. A. C. Stuart, W. T. S. Huck, J. Genzer, M. Müller, C. Ober, M. Stamm, G. B. Sukhorukov, I. Szleifer, V. V. Tsukruk, M. Urban, F. Winnik, S. Zauscher, I. Luzinov, and S. Minko, Nat. Mater. **9**, 101–113 (2010).
[174] R. C. Schroden, M. Al-Daous, C. F. Blanford, and A. Stein, Chem. Mater. **14**, 3305 (2002).
[175] P. Theato, B. S. Sumerlin, R. K. O'Reilly, and T. H. Epps, III, Chem. Soc. Rev. **42**, 7055 (2013).
[176] T. Skylar, Architectural Design **84**, 116 (2014).
[177] Z. Hao, W. Piotr, P. Camilla, M. Daniele, B. Matteo, and W. D. Sybolt, Adv. Mater. **27**, 3883 (2015).
[178] D. Martella, D. Antonioli, S. Nocentini, D. S. Wiersma, G. Galli, M. Laus, and C. Parmeggiani, RSC Adv. **7**, 19940 (2017).
[179] F. Momeni, S. M. M. H. N, X. Liu, and J. Ni, Materials and Design **122**, 42 (2017).
[180] N. Akihiro, M. Ahmed, Z. Hang, and M. Martin, Adv. Sci. **5**, 1700038 (2017).
[181] P. Haedong, K. Hyungho, A. Yongsan, Y. Woong-Ryeol, M. Myoung-Woon, and H. Kahyun, Phys. Status Solidi (RRL) **12**, 1800040.
[182] O. Hess, J. B. Pendry, S. A. Maier, R. F. Oulton, J. M. Hamm, and K. L. Tsakmakidis, Nat. Mater. **11**, 573 (2012).
[183] I. Shadrivov, M. Lapine, and Y. Kivshar, *Nonlinear, Tunable and Active Metamaterials*, Springer Series in Materials Science (Springer International Publishing, 2014).
[184] K. Fan and W. J. Padilla, Mater. Today **18**, 39 (2015).
[185] X. Tong, *Functional Metamaterials and Metadevices*, Springer Series in Materials Science (Springer International Publishing, 2017).
[186] S. Rout and S. Sonkusale, *Active Metamaterials: Terahertz Modulators and Detectors* (Springer International Publishing, 2017).
[187] K. Yu, N.-X. Fang, G. Huang, and Q. Wang, Adv. Mater. **30**, 1706348 (2018).
[188] J. S. Nicholas A. Estep, Dimitrios L. Sounas and A. Alu, Nat. Phys. **10**, 923–927 (2014).
[189] M. Ozaki, Y. Shimoda, M. Kasano, and K. Yoshino, Adv. Mater. **14**, 514–518 (2002).
[190] M. Kamenjicki, I. Lednev, and S. A. Asher, Adv. Funct. Mater. **15** (2005).
[191] T. J. Cui, M. Q. Qi, X. Wan, J. Zhao, and Q. Cheng, Light Sci. Appl. **3**, e218 (2014).
[192] Z. Jie *et al.*, arXiv:1806.04414 (2018).
[193] N. Courjal, S. Benchabane, J. Dahdah, G. Ulliac, Y. Gruson, and V. Laude, Appl. Phys. Lett. **96**, 131103 (2010).

[194] D. Shin, J. Kim, C. Kim, K. Bae, S. Baek, G. Kang, Y. Urzhumov, D. R. Smith, and K. Kim, Nat. Commun. **8**, 16090 (2017).
[195] J. M. Weissman, H. B. Sunkara, A. S. Tse, and S. A. Asher, Science **274**, 959–963 (1996).
[196] S. Kubo, Z.-Z. Gu, K. Takahashi, A. Fujishima, H. Segawa, and O. Sato, J. Am. Chem. Soc. **126**, 8314 (2004).
[197] D. Roy, J. N. Cambre, and B. S. Sumerlin, Prog. Polym. Sci. **35**, 278 (2010), special Issue on Stimuli-Responsive Materials.
[198] D. H. Gracias, Current Opinion in Chemical Engineering **2**, 112 (2013).
[199] V. Laude, A. Belkhir, A. F. Alabiad, M. Addouche, S. Benchabane, A. Khelif, and F. I. Baida, Optica **4**, 1245 (2017).
[200] S. Babaee, N. Viard, P. Wang, N. X. Fang, and K. Bertoldi, Adv. Mater. **28**, 1631–1635 (2016).
[201] Z. Nicolaou and A. Motter, Nat. Mater. **11**, 608 (2012).
[202] J. Qu, M. Kadic, A. Naber, and M. Wegener, Sci. Rep. **7**, 40643 (2017).
[203] H. Zhang, X. Guo, J. Wu, D. Fang, and Y. Zhang, Sci. Adv. **4**, 8535 (2018).
[204] X. Zhang, J. Liu, M. Chu, and B. Chu, Appl. Phys. Lett. **109**, 072903 (2016).
[205] M. Kamenjicki, I. k. Lednev, A. Mikhonin, R. Kesavamoorthy, and S.-A. Asher, Adv. Funct. Mater. **13** (2003).
[206] V. Bacot, M. Labousse, A. Eddi, M. Fink, and E. Fort, Nature Physics **12**, 972 (2016).
[207] Deck-Léger, Zoé-Lise, Akbarzadeh, Alireza, and C. Caloz, Phys. Rev. B **97**, 104305 (2018).
[208] J. C. Halimeh, R. T. Thompson, and M. Wegener, Phys. Rev. A **93**, 013850 (2016).
[209] K. Fang, Z. Yu, and S. Fan, Nature Photon. **6**, 782 (2012).
[210] H. Nassar, H. Chen, A. N. Norris, and G. L. Huang, Phys. Rev. B **97**, 014305 (2018).
[211] S. Xu and C. Wu, Phys. Rev. Lett. **120**, 096401 (2018).